

Received 22 April 2024, accepted 30 April 2024, date of publication 3 May 2024, date of current version 14 May 2024.

Digital Object Identifier 10.1109/ACCESS.2024.3396497

## RESEARCH ARTICLE

# Throughput Maximization of Wireless Powered IoT Network With Hybrid NOMA-TDMA Scheme: A Genetic Algorithm Approach

ABID AFRIDI<sup>1</sup>, IQRA HAMEED<sup>2</sup>, CARLA E. GARCÍA<sup>3</sup>, (Member, IEEE), AND INSOO KOO<sup>1</sup>

<sup>1</sup>Department of Electrical, Electronic and Computer Engineering, University of Ulsan, Ulsan 44610, South Korea

<sup>2</sup>Department of Electronic Engineering, Hanyang University, Seoul 04763, South Korea

<sup>3</sup>Interdisciplinary Centre for Security, Reliability and Trust, University of Luxembourg, Luxembourg City 1209, Luxembourg

Corresponding author: Insoo Koo (iskoo@ulsan.ac.kr)

This work was supported by the Regional Innovation Strategy (RIS) through the National Research Foundation of Korea (NRF) funded by the Ministry of Education (MOE) under Grant 2021RIS-003.

**ABSTRACT** In this study, we explore a hybrid non-orthogonal multiple access and time division multiple access (NOMA-TDMA) approach designed to maximize sum throughput in a wireless powered Internet of Things (IoT) network (WPIN). Hybrid access points send energy signals to users on downlink, and users in various groups utilize that harvested energy to transmit information on uplink. This process is facilitated by the NOMA-TDMA scheme wherein users of the same group use NOMA for simultaneous transmissions, and separate time slots are assigned to each group through TDMA. Under this hybrid NOMA-TDMA scheme, the main objective is to enhance the network's sum throughput by jointly optimizing both the allocation of time for downlink and uplink and the downlink beamforming vectors. Given the complex interdependence of variables, the problem is inherently non-convex, making it difficult to solve numerically. Therefore, we reformulate the problem as a bi-level programming problem—the outer-level sub-problem addresses beamforming vectors using a genetic algorithm while the inner-level sub-problem deals with the allocation of downlink and uplink time through the Lagrange multiplier method. Numerical results show that the proposed hybrid NOMA-TDMA scheme outperforms baseline schemes like orthogonal multiple access and equal time allocation, in terms of the sum throughput of the WPIN.

**INDEX TERMS** Internet of Things (IoT), wireless powered IoT network (WPIN), multiple input single output (MISO), wireless energy transfer (WET), wireless information transfer (WIT), energy harvesting, non-orthogonal multiple access (NOMA), orthogonal multiple access (OMA), genetic algorithm (GA), Lagrange multiplier (LM).

## I. INTRODUCTION

The Internet of Things (IoT) represents an integrated network of intelligent devices capable of interacting and collaborating through the Internet with each other, with humans, and with the environment. This convergence facilitates a seamless bridge between the physical and digital realms, empowering objects with capabilities to execute complex tasks independently. A crucial aspect of the IoT is its inherent autonomy, which requires minimal to no human

intervention for operational functionality [1]. The IoT has significantly enhanced the scope of application domains like transportation, smart grids, security, public safety, agriculture, logistics, and e-health with its distinctive and unparalleled features [2].

The IoT holds the potential to profoundly impact various aspects of our daily lives, offering significant advantages to businesses through the automation of processes and enhanced management of environmental factors [3]. Conventionally, sensor networks and other low-energy wireless networks are powered by fixed energy sources like batteries, which have finite operating times [4]. Even though changing

The associate editor coordinating the review of this manuscript and approving it for publication was Patrizia Liveri<sup>1</sup>.

or recharging the batteries might prolong the network's lifespan, doing so can be difficult, expensive, risky (e.g., in harmful environments), or nearly impossible (e.g., sensors inserted into human bodies) [5]. In addition, widespread implementation of the IoT presents considerable challenges, such as security vulnerabilities, data privacy concerns, and scalability. Among these, energy limitations are one of the main challenges to its acceptance.

Wireless power transfer (WPT) has been considered an important technology in recent years, not only due to its ease of use and enhanced security but also because of its continually evolving renewable features. WPT has become integral to various applications, including mobile charging, electric vehicles, IoT networks and implantable medical devices [6]. To overcome the energy limitation on IoT networks, harvesting energy from the environment has attracted a lot of attention lately as a viable alternative for extending the lifespan of wireless networks [7], [8]. Since radio frequency (RF) signals can be obtained from specialized transmitters that already meet the requirements for far-field wireless power transfer, they are drawing greater attention than other energy sources [9], [10], [11].

In recent years, wireless powered IoT networks (WPINs) have surfaced as a significant advancement for battery-life-constrained mobile and communications devices [9]. This technology has been identified as a crucial solution for several low-power scenarios, including wireless powered communication networks (WPCNs) and radio frequency identification (RFID) networks [12]. Typically, WPINs consist of a hybrid access point (H-AP) that coordinates multiple wireless devices for wireless energy transfer on downlink and wireless information transfer on uplink. Furthermore, in WPINs, the harvest-then-transmit (HTT) protocol is considered wherein wireless devices operate without battery power. Instead, they harvest energy from the H-AP and utilize this energy to send information [9], [13]. To ensure effective operation and performance of a network, WPINs require cooperative design in information and energy transmissions. In WPINs where the H-AP is equipped with multi-antenna configurations, the technique of energy beamforming—concentrating RF signals into a focused beam—significantly enhances the efficiency of energy transmissions [14]. In addition, WPINs can benefit from energy beamforming at the H-AP since a multi-antenna H-AP can manage the transmit beamforming vectors, improving energy transmission efficiency. Moreover, through the strategic design of energy beams, it is possible to improve the uplink throughput for each user. This enhancement stems from the increased energy harvested on downlink, which in turn permits higher transmit power on uplink [15].

Alongside this, non-orthogonal multiple access (NOMA) has been introduced as a strategy to facilitate connectivity of a massive number of devices within IoT networks. NOMA allows numerous users to share a single (frequency, time, coding, or spatial) channel at the same time, resulting in improved spectrum efficiency and energy efficiency [16]. From the perspective of IoT networks, the spectral efficiency

holds considerable importance in the 6G wireless networks. In the absence of efficient spectrum allocation schemes, the densification of devices would ultimately saturate the spectral resources of 6G networks, leading to network-wide disruptions [17]. NOMA is considered a promising resources allocation scheme in IoT networks, [18], [19]. According to a study by Ding et al. [20], NOMA can obtain a higher uplink sum rate than orthogonal multiple access (OMA). However, compared to OMA, NOMA requires substantially greater receiver complexity when employing successive interference cancellation (SIC) [21]. Additionally, the involvement of a large number of users in the SIC process introduces a performance-limiting factor attributed to error propagation resulting from the removal of prior users' signals. Although NOMA may not consistently exceed the performance of OMA, like time division multiple access (TDMA) in certain scenarios, OMA can exhibit superior energy efficiency compared to NOMA in WPCNs [22]. Consequently, finding a trade-off between complexity and performance in WPINs is still a challenge.

#### A. RELATED WORKS

The literature features a wide range of studies that have explored Wireless Powered IoT Networks (WPINs), [9], [23], [24], [25], [26], [27], [28], NOMA based WPINs [29], [30], [31], [32], [33], [34] and hybrid NOMA-TDMA based WPINs [35], [36], [37], [38].

In the study by Ju and Zhang [23], the authors delved into throughput maximization in wireless powered communication networks by utilizing the HTT protocol. They proposed an optimal solution aimed at enhancing throughput by strategically allocating time to wireless users. Furthermore, they addressed (and proposed a solution for) the doubly near-far problem by optimizing common throughput, offering significant insights into improving network efficiency.

Asiedu et al. provided a study on beamforming and allocation of resources for multi-user full duplex wireless powered communications in IoT networks [24]. This research explored a MISO system configuration where the AP functions in full duplex mode with the users in half duplex mode. Optimization of channel assignment, time resources, and power allocation is undertaken to improve the uplink weighted sum rate.

Zheng et al. addressed maximizing throughput based on data packets in their study [26]. They proposed both short- and long-term throughput maximization in mobile WPINs. They segmented the short-term problem based on data packet generation, and introduced a generated-data-packets throughput-maximization algorithm. For long-term maximization, they demonstrated its equivalence to the integer knapsack problem, and developed a deep deterministic policy gradient (DDPG) multi-node resource allocation (DMRA) algorithm to determine optimal times, power allocations, and channel assignments among IoT users.

In [9], the authors focused on simultaneously optimizing transmission time and packet error rate for each user to

either maximize total effective throughput or minimize overall transmission time, subject to users' individual effective-amount-of-information requirements.

Yang et al. proposed a study on maximizing minimum throughput in wirelessly powered IoT systems assisted by backscatter technology [28]. The objective of this research was to establish a transmission schedule for all devices that would maximize the system's minimum throughput. In [29], Zewde and Gursoy provided a study on the efficacy of NOMA in wireless powered communications. Their aim was to enhance a system's energy efficiency when using NOMA for uplink information transfer. The investigation focused on numerous energy-harvesting UEs operating under the HTT protocol. For uplink information transfer, power-domain multiplexing was employed, and the receiver was designed to decode each UE's information in a way that allows the UE with the highest channel gain to be decoded without interference.

Zhai et al. investigated the non-orthogonality of NOMA in intracell interference [30]. To coordinate intracell interference, they proposed a solution to dynamic user scheduling and the power allocation problem with the objective being to minimize total power consumption of the whole network under constraints on all users' long-term requirements.

In [31], Rauniyar et al. explored the dynamics of radio frequency energy harvesting and information transfer by leveraging time switching relaying (TSR), power splitting relaying (PSR), and NOMA with the objective of optimizing sum throughput. The study describes a process where a power-limited IoT relay node initially harvests energy from the RF signal of a source node through either TSR or PSR. Subsequently, it transmits information from the source node together with its own data to the designated destination nodes using the NOMA protocol.

Wang et al. proposed a study on throughput maximization for peer-assisted wireless powered IoT NOMA networks [32]. The objective of this research was to maximize the sum-throughput of each proposed model, while considering the combination of TDMA and NOMA, under the assumption that the power of active UEs is fixed. This study states different transmission modes (non-stand-alone/stand-alone) and different operations (NOMA/NOMA-plus-TDMA) and re-investigate the above schemes in the scenario where active UEs' energy is limited, i.e., the power of active UEs is not fixed and is affected by time allocation.

In the study by Tegos et al. [33], they explored two random access (RA) protocols that enhance the traditional slotted ALOHA (SA) by integrating it with uplink NOMA. Compared to other RA protocols, SA is favored for its low complexity and its ability to eliminate partially overlapping transmissions, thereby reducing collisions. However, SA can become inefficient under conditions of high traffic load and increased device numbers, leading to congestion. To address these issues, this study introduces two detection techniques aimed at mitigating interference when two sources transmit simultaneously in the same time slot. These techniques SIC

with an optimal decoding order policy and joint decoding (JD) are designed to decrease the number of collisions and enhance the throughput of SA while maintaining system simplicity.

Manzoor et al. investigated the combination of NOMA using power-domain with backscatter communication (BC) [34]. The goal of this work was to maximize the total energy efficiency (EE) of the IoT network, subject to the quality of services of each IoT device. This study introduced a BC in a multicell IoT network, where a source in each cell transmits a superimposed signal to its associated IoT devices using NOMA. The backscatter sensor tag (BST) also transmits data to IoT devices by reflecting and modulating the superimposed signal of the source. The proposed work simultaneously optimizes the total power of each source, power allocation coefficient of IoT devices, and RC of BST under imperfect SIC decoding.

The authors in [36] discussed maximization of the weighted sum rate for TDMA and NOMA by optimizing harvesting time and transmission time variables. In [37], a hybrid approach combining NOMA and TDMA for intelligent reflecting surface (IRS)-assisted wireless powered communications was studied. Users were organized into various clusters to harvest energy on downlink, followed by transmission of information to the base station (BS) by utilizing a combined NOMA and TDMA strategy on uplink.

## B. MOTIVATION AND CONTRIBUTIONS

Motivated by the aforementioned research, we studied the sum-throughput problem for wireless powered IoT networks. We studied the efficiency and the diverse applications of NOMA in WPINs; however, studies on hybrid NOMA-TDMA schemes were not found in the literature review. The primary motivation for selecting TDMA alongside NOMA in this study is due to TDMA's simplicity and its proven effectiveness in managing interference between users in wireless networks [39]. TDMA organizes transmission times into distinct slots for different user groups [35]. This clear structure simplifies scheduling and reduces the complexity of system design, which is particularly beneficial when combined with NOMA's power-domain multiplexing [40]. As a generalization of both NOMA and TDMA systems, hybrid NOMA-TDMA reduces the complexity of SIC implementation while simultaneously providing more degrees of freedom to enhance performance. Additionally, TDMA is well-suited for situations where it's important to synchronize user transmissions and minimize system overhead [41]. Its straightforward implementation, supported by well-established technologies and infrastructure, makes TDMA a practical choice for both theoretical research and real-world applications. To solve this non-convex problem, we converted the optimization problem of hybrid NOMA-TDMA to a bi-level programming problem with outer and inner sub-problems. The non-convex problem is complex due to coupling of highly optimal variables.

**TABLE 1.** Notations used for mathematical expressions.

Symbols	Definitions
$(\mathbf{b})^H$	The conjugate transpose of complex-valued vector $\mathbf{b}$
$\mathbb{C}^{m \times n}$	The space of $m \times n$ complex-valued matrices
$i$	An imaginary unit, i.e., $i^2 = -1$
$ \beta $	The absolute value of complex-valued scalar $\beta$
$\text{Tr}(\mathbf{B})$	The trace of matrix $\mathbf{B}$
$\text{diag}(\mathbf{b})$	The diagonal matrix of vector $\mathbf{b}$
$\text{rank}(\mathbf{B})$	The rank of matrix $\mathbf{B}$
$x \in \mathbf{B}$	$x$ is an element in set $\mathbf{B}$
$\mathbf{B} \succeq 0$	Positive semidefinite matrix $\mathbf{B}$
$[\mathbf{B}]_{m,n}$	The element in matrix $\mathbf{B}$ at the $m_{th}$ row and $n_{th}$ column

We solve the outer problem using a genetic algorithm, and solve the inner problem by means of the Lagrangian method.

The main contributions of our paper are as follows.

- We propose a hybrid NOMA-TDMA MISO system for sum-throughput maximization in WPINs by jointly optimizing the downlink beamforming vectors and uplink and downlink time, subject to minimum harvested energy.
- To solve the non-convex problem, we propose transforming it into a bi-level programming problem that consists of an outer problem and an inner problem. Hence, the main problem turns into sub-problems, and we solve the outer sub-problem for beamforming vectors with a genetic algorithm and solve the inner problem for downlink and uplink time allocation by using the Lagrange multiplier method to find the near-optimal solution.
- As a comparative scheme, we consider OMA and equal time allocation (ETA) techniques and evaluate the performance of the proposed scheme via simulations that demonstrate the proposed hybrid NOMA-TDMA scheme has better performance than other conventional scenarios and OMA techniques.

This paper's remaining sections are arranged as follows: In Section II, we discuss the system model and problem formulation for sum-throughput maximization. Section III describes the proposed solution for bi-level programming, which consists of genetic algorithm (GA) and the Lagrange multiplier method. Section IV explains the numerical results and discussion for evaluation and comparison purposes. Finally, conclusions are discussed in Section V.

Table 1 provides a list of important notations and their definitions.

## II. SYSTEM MODEL AND PROBLEM FORMULATION

We consider a multiple input single output transmission system that consists of a hybrid access point and  $N$  distributed IoT users in  $K$  groups, as shown in Fig. 1. The H-AP is equipped with multiple antennae,  $M > 1$ , and users are equipped with a single antenna each.  $\mathbf{H}_1, \mathbf{H}_2, \mathbf{H}_3, \dots, \mathbf{H}_K$  represent channel conditions between the H-AP and each user group. These coefficients characterize the quality of the channel, including aspects like path loss and fading, which affect both energy transfer and data transmission processes.

The users' grouping strategy involves arranging them as  $U_1, \dots, U_N$  such that  $\|\mathbf{h}_1\| \geq \|\mathbf{h}_2\| \geq \dots \geq \|\mathbf{h}_N\|$ , where  $\mathbf{h}_n$  denotes the channel coefficient from  $n_{th}$  user to the H-AP, for  $n = 1, 2, \dots, N$ . This method of grouping is referred to as large-channel-strength difference (LCSD), which lets the user—H-AP channel strength differences among users in the same group stay as large as possible [37], [42]. User groups under this scheme can be  $\{U_1, U_4, U_7, U_{10}\}$ ,  $\{U_2, U_5, U_8, U_{11}\}$ , and  $\{U_3, U_6, U_9, U_{12}\}$ . The H-AP sends energy to users on downlink by using beamforming, whereas users transmit information to the H-AP on uplink by utilizing the harvested energy. We have  $N$  distributed users and  $K$  groups where  $n = \{1, 2, \dots, |N|\}$  and  $k = \{1, 2, \dots, |K|\}$ . The hybrid NOMA-TDMA scheme switches to TDMA when  $K = N$ , and uses NOMA when  $K=1$  [37].

We also assume that channel state information is known at the H-AP. The time frame is divided such that the first part is  $\tau_0$  where  $(0 < \tau_0 < 1)$  where the H-AP broadcasts wireless energy on downlink to all users. All users have initial power ( $P_i = 0$ ), recharging themselves with the energy from the H-AP to transmit information under the HTT protocol. Uplink time is further divided using TDMA to assign a time slot to each group, in which all users of that group transmit information simultaneously on uplink to the H-AP. The amount of time assigned to the  $k_{th}$  group on uplink is denoted  $\tau_k$  ( $0 < \tau_k < 1$ ), as shown in Fig. 2.

Nevertheless, the perfect channel estimation is challenging but there are some preliminary studies have been done on channel estimation of IoT networks. In [43], the author proposed two models relevant to low powered LP-IoT communication in IoT networks. The first model provided a theoretical representation of the wireless channel for the LP-IoT network while the second model was the channel estimation model, where they applied the least squares (LSE) and maximum likelihood (MLE) techniques to estimate the LP-IoT wireless channel. Reference [44] investigated the channel estimation performance of massive multiple-input-multiple-output (MIMO) IoT systems with Rician fading. This framework utilized the LS and minimum mean squared error (MMSE) estimation methods and considered the relative channel estimation error (RCEE) between the IoT device and base-station, and provide the approximations of the expectation of RCEE. In a study [45], the author proposed a model-driven deep learning algorithm for joint activity detection and channel estimation based on the principle of approximate message passing (AMP) which does not require the prior information about active probabilities and channel variance, and can significantly improve the performance with a finite number of training data.

## A. DOWNLINK TRANSMISSION

During the downlink phase, the H-AP transmits an arbitrary energy signal in the form of beams directed towards users with beamforming vector  $\mathbf{w}$  at time  $\tau_0$ . Since a distant user from the H-AP receives less power on downlink and suffers

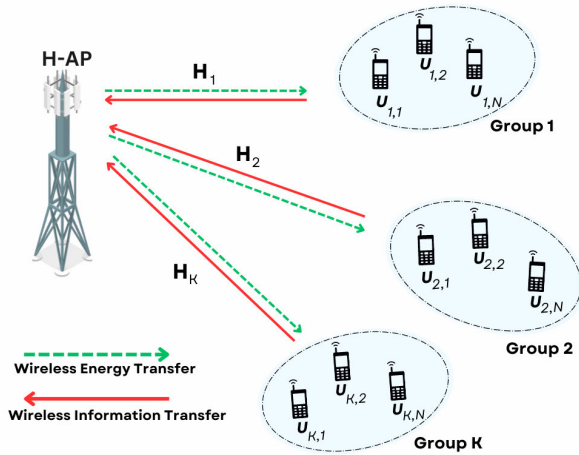


**FIGURE 1.** The wireless powered IoT network with WET on downlink to all users and WIT on uplink using the proposed hybrid NOMA-TDMA.

from throughput degradation on uplink compared to a nearby user, the H-AP applies different energy beamforming weights to control power allocation. We denote the downlink energy signal as  $s_{dl} = \mathbf{w}s_0$ , where  $s_0$  is an independent and identically distributed random signal with zero mean and unit variance, and  $\mathbf{w} \in C^{M \times 1}$  denotes the energy beamformers for the transmitter. The transmit power of the H-AP on downlink can be expressed as  $E[|s_{dl}|^2] = |\mathbf{w}|^2$ . The H-AP has a transmit sum-power constraint,  $P_{max}$ ; thus, we have  $|\mathbf{w}|^2 \leq P_{max}$ . The signal received from the H-AP by the  $n_{th}$  user in the  $k_{th}$  group is represented as follows:

$$y_{(k,n)} = \mathbf{h}_{(k,n)}^H \mathbf{w}s_0 + z_n \quad (1)$$

where  $\mathbf{h}_{k,n} \in C^{M \times 1}$  is the link from the H-AP (M antennae) to the  $n_{th}$  user in the  $k_{th}$  group;  $z_n$  is noise from the  $n_{th}$  user, whereas  $\mathbf{w} \in C^{M \times 1}$  denotes the energy beamforming vector at the H-AP.

We assume that the energy harvested from the receiver's noise is negligible in comparison to the energy harvested from the energy signal, so we ignore receiver noise in further problem formulations. Then, the amount of energy harvested by the  $n_{th}$  user in the  $k_{th}$  group is

$$^*E_{k,n} = \xi_{k,n} |\mathbf{h}_{k,n}^H \mathbf{w}|^2 \tau_0 \quad (2)$$

where  $0 < \xi_{k,n} < 1$  is the energy-harvesting efficiency of the  $n_{th}$  user in the  $k_{th}$  group, and  $\tau_0$  is the time taken for downlink energy transfer.

## B. UPLINK TRANSMISSION

After harvesting energy during the downlink phase, users send information during the uplink phase by using the harvested energy. We consider a hybrid scheme for information transfer on uplink where different groups transmit at different times using TDMA, while users in the same group transmit at the same time using NOMA. For users under NOMA, we assume effective channel gain for users in the  $k_{th}$  group is denoted in descending order:  $\|\mathbf{h}_{k,1}\|^2 > \|\mathbf{h}_{k,2}\|^2 > \|\mathbf{h}_{k,3}\|^2 > \dots > \|\mathbf{h}_{k,n}\|^2$ . Using TDMA, each

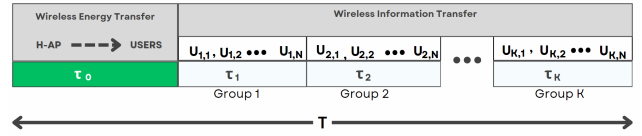


**FIGURE 2.** Time-frame divisions for downlink energy transfer and uplink information transfer.

group is allocated a single time slot for uplink transmission. Then, the available average power of the  $n_{th}$  user in the  $k_{th}$  group to transmit on uplink can be expressed as

$$P_{k,n} = \frac{E_{k,n}}{\tau_k} = \frac{\xi_{k,n} |\mathbf{h}_{k,n}^H \mathbf{w}|^2 \tau_0}{\tau_k} \quad (3)$$

We assume users have no other energy source or battery to store harvested energy, and hence, all energy must be used for transmission [48], [49]. The signal received at the H-AP from the  $n_{th}$  user in the  $k_{th}$  group can be written as follows:

$$r_{k,n} = \mathbf{v}_n^H \mathbf{h}_{k,n} s_{ul} + z \quad (4)$$

where  $\mathbf{v}_n \in C^M \times 1$  denotes the receiver beamforming vector that is used to decode the information of the  $n_{th}$  user;  $s_{ul} = \sqrt{p_{k,n}} s_{k,n}$  denotes the information signal on uplink, and  $z$  is noise at the H-AP. According to NOMA principles, for uplink employing SIC at the H-AP, the decoding process is executed in descending order. In this decoding order, the first user needs to endure all in-group interference from the other users, but a user later in the decoding order can benefit from the throughput by cancelling the interference, and the weakest user's message is decoded without interference. The signal-to-interference-plus-noise ratio is then calculated as the ratio of the desired signal power to the total interference plus noise, which is expressed as

$$\gamma_{k,n} = \frac{p_{k,n} |\mathbf{v}_n^H \mathbf{h}_{k,n}|^2}{\sum_{i=n+1}^N p_{k,i} |\mathbf{v}_i^H \mathbf{h}_{k,i}|^2 + \sigma^2}, \quad 1 \leq n \leq N-1 \quad (5)$$

so the signal-to-noise ratio for the  $N_{th}$  user can be written as

$$\gamma_{k,n} = \frac{p_{k,n} |\mathbf{v}_n^H \mathbf{h}_{k,n}|^2}{\sigma^2}, \quad N_{th} \text{ user} \quad (6)$$

We adopt maximal ratio combining (MRC) beamforming at the receiver as described in [50], where beamforming vector  $\mathbf{v}_n$  is defined as  $\mathbf{v}_n = \frac{\mathbf{h}_{k,n}}{\|\mathbf{h}_{k,n}\|}$ . Furthermore, acknowledging that all harvested energy is utilized for uplink transmission, we adjust uplink transmit power to reflect the harvested energy. Consequently, equation (5) can be reformulated as follows:

$$\gamma_{k,n} = \frac{\frac{\tau_0}{\tau_k} \xi_{k,n} |\mathbf{h}_{k,n}^H \mathbf{w}|^2 \|\mathbf{h}_{k,n}\|^2}{\sum_{i=n+1}^N p_{k,i} |\mathbf{v}_i^H \mathbf{h}_{k,i}|^2 + \sigma^2}, \quad 1 \leq n \leq N-1 \quad (7)$$

Equation (6) is also updated under MRC as

$$\gamma_{k,n} = \frac{\frac{\tau_0}{\tau_k} \xi_{k,n} |\mathbf{h}_{k,n}^H \mathbf{w}|^2 \|\mathbf{h}_{k,n}\|^2}{\sigma^2}, \quad N_{th} \text{ user} \quad (8)$$

Using Shannon’s capacity formula, the throughput of the  $n_{th}$  user in the  $k_{th}$  group can be written as

$$R_{k,n} = (\tau_k) \log_2(1 + \gamma_{k,n}) \quad (9)$$

Hence, the sum throughput for the  $k_{th}$  group can be written as expressed in [51]:

$$R_k = (\tau_k) \log_2\left(1 + \frac{\sum_{n=1}^N \frac{\tau_0}{\tau_k} \xi_{k,n} |\mathbf{h}_{k,n}^H \mathbf{w}|^2 \|\mathbf{h}_{k,n}\|^2}{\sigma^2}\right) \quad (10)$$

In this problem, to maximize the sum throughput of all users while jointly optimizing downlink beamforming vector  $\mathbf{w}$  and allocation of time  $\tau$  for downlink and uplink, we formulate the optimization problem as follows:

$$(P1) : \max_{\mathbf{w}, \tau} \sum_{k=1}^K R_k \quad (11a)$$

$$\text{s.t. } C_1 : \xi_{k,n} |\mathbf{h}_{k,n}^H \mathbf{w}|^2 \tau_0 \geq e_{min} \quad (11b)$$

$$C_2 : \|\mathbf{w}\|^2 \leq P_{max} \quad (11c)$$

$$C_3 : 0 \leq \sum_{k=0}^K \tau_k \leq 1 \quad (11d)$$

where  $e_{min}$  is the minimum threshold for harvested energy, and  $\mathbf{w}$  is the beamforming vector. Constraint  $C_1$  ensures quality of service for users in order to satisfy the minimum criteria for harvested energy in the downlink phase. Moreover, constraint  $C_2$  guarantees that the H-AP’s transmit power does not exceed the maximum available power, and constraint  $C_3$  fulfills time-frame normalization for time allocation.

Since  $P1$  is non-convex and highly complex because of the coupling of optimal variables aimed at maximizing sum throughput, finding a feasible solution analytically is difficult. In this paper, we convert  $P1$  into a bi-level programming problem consisting of outer-level variables and inner-level variables in order to get a tractable solution.

### III. PROPOSED SOLUTION OF BI-LEVEL PROGRAMMING PROBLEM

Based on problem  $P1$ , we can see that it is extremely intricate and challenging to solve because of the highly coupled variables and non-convexity of the objective functions and constraints. Therefore, to solve  $P1$ , we convert it to a bi-level programming problem comprising outer-level and inner-level variables,  $\{\mathbf{w}\}$  and  $\tau$ , respectively.

#### A. OUTER-LEVEL VARIABLE

$$(P2) : \max_{\mathbf{w}} \sum_{k=1}^K R_k \quad (12a)$$

$$\text{s.t. } C_1 : \xi_{k,n} |\mathbf{h}_{k,n}^H \mathbf{w}|^2 \tau_0 \geq e_{min} \quad (12b)$$

$$C_2 : \|\mathbf{w}\|^2 \leq P_{max} \quad (12c)$$

Problem  $P2$  describes the outer-level problem, which deals with downlink beamforming vectors  $\{\mathbf{w}_0\}$ . We consider a

scheme based on a genetic algorithm (GA) to ascertain the outer-level variable values. The GA is recognized for its efficacy in solving linear and non-linear problems, and excels at avoiding local minima to attain solutions that are close to optimal through the utilization of selection, crossover, and mutation techniques.

#### B. INNER-LEVEL VARIABLE

$$(P3) : \max_{\tau} \sum_{k=1}^K R_k \quad (13a)$$

$$\text{s.t. } C_1 : \sum_{k=0}^K \tau_k \leq 1, \quad \tau_k > 0, k = 0, 1, \dots, K. \quad (13b)$$

where Problem  $P3$  corresponds to an inner-optimization problem with respect to variable  $\tau$ , which shows the time for downlink and uplink transmissions. In addition, the constraint ensures that the downlink and uplink times must be less than or equal to 1. Since Problem  $P3$  is convex, we propose a Lagrange multiplier algorithm to determine the optimal value of the inner-level variable.

The methodology proposed in this study employs a cyclical optimization process for both the upper-level variables  $\{\mathbf{w}\}$  and the inner-level variables  $\{\tau\}$ . Initially, a GA-based framework is introduced to determine the values of outer-level variables  $\{\mathbf{w}\}$ . After that, the Lagrange multiplier method is applied to the inner optimization problem using the values of  $\{\mathbf{w}\}$  to achieve close to optimal solutions for the inner-level variable represented by  $\{\tau\}$ . Objective function (10a) is then evaluated, and the GA uses the result to further refine variable set  $\{\mathbf{w}\}$ . The process iterates with the updated  $\{\mathbf{w}\}$  values informing the Lagrange multiplier’s adjustment of the  $\{\tau\}$  variables, continuing until convergence is achieved. The GA framework is described in Section III-B1, while implementation of the Lagrange multiplier technique is explained in Section III-B2 and Section III-B3 describes the complexity analysis.

#### 1) OUTER-LEVEL SUB-PROBLEM SOLUTION USING A GENETIC ALGORITHM

In this subsection, we solve the outer sub-problem of the bi-level programming problem to find the optimal values for beamforming vector  $\mathbf{w}$  by fixing another variable, like time allocations  $\{\tau_0, \tau_1, \tau_2, \dots, \tau_k\}$ . To solve Problem  $P2$ , we use a genetic algorithm. The GA represents a class of optimization methodologies derived from the principles of natural selection and genetics. The genetic algorithm begins with an initial population where individual solutions evolve through selection and mutation processes. The aim is to evolve into a solution that optimally satisfies the cost function [52]. Broadly, GAs are categorized into two types: binary and continuous. The binary GA operates on binary strings, encoding the problem’s variables into binary format and optimizing the objective function in this discrete space.

On the other hand, the continuous GA, also referred to as a real-coded GA, works directly with continuous variables, thus offering a more direct approach to optimizing the objective function. Due to the absence of a decoding step for chromosome evaluation, the continuous GA typically exhibits higher efficiency than its binary counterpart. In the context of our study, particularly in addressing beamforming problems, we adopt the continuous GA approach. This decision stems from the increased efficiency gained by operating directly on real-valued variables, bypassing the need for encoding and decoding inherent in the binary GA.

In a GA, the population comprises  $N_{\text{pop}}$  chromosomes where each  $n_{\text{th}}$  chromosome, denoted as  $cr_n$ , contains  $N_{\text{var}}$  variables. Therefore, a chromosome can be articulated as  $cr_n = [w_1, \dots, w_{N_{\text{var}}}]$  for  $n = 1, \dots, N_{\text{pop}}$ . The efficacy of each chromosome is quantified through a cost function, which is defined by objective function (12a). The process initiates with a natural selection phase, during which chromosomes are ranked in descending order based on their cost, represented as  $f(cr_n)$ . Following this ranking, only a portion of the population, predetermined by selection rate  $\{SelRate\}$ , is preserved for subsequent generations. The retained chromosomes will be used as parents for crossover and mutation operations in the genetic algorithm:

$$N_{\text{keep}} = \lfloor SelRate N_{\text{pop}} \rfloor, \quad (14)$$

where  $N_{\text{keep}}$  denotes the quantity of chromosomes retained for generating new offspring, and  $N_{\text{pop}} - N_{\text{keep}}$  determines the chromosomes that are eliminated. Following this, the pairing procedure entails selection of chromosomes from the conserved pool of  $N_{\text{keep}}$  chromosomes, with the aim of forming  $MatP = \frac{N_{\text{pop}} - N_{\text{keep}}}{2}$  mating pairs. The selection process employs a rank weighting method wherein the probability for the  $n_{\text{th}}$  chromosome is determined as follows:

$$Pb_n = \frac{N_{\text{keep}} - n + 1}{\sum_{n=1}^{N_{\text{keep}}} n}, \quad n = 1, \dots, N_{\text{keep}}. \quad (15)$$

Considering that probability, the initial step involves arranging the chromosomes in a descending sequence based on their cost, thereby positioning the chromosome with the highest cost at the top. Following this, we proceed to ascertain the cumulative probabilities for each chromosome, denoted by  $CPb_n = \sum_{i=1}^n Prob_i$ . To select the first parent,  $parent_{x_1}$ , for each mating pair indexed by  $x$  (where  $x = 1, \dots, MatP$ ), a uniformly distributed random value,  $rand_{x_1}$  within  $[0, 1]$ , is generated. Initiating from  $n = 1$  within the assortment of the mating pool, we select the earliest chromosome where the cumulative probability,  $CPn$ , is greater than  $rand_{x_1}$ , appointing it as  $parent_{x_1}$  for the  $x_{\text{th}}$  mating pair. Subsequently, a second random value,  $rand_{x_2}$ , is generated to determine the second parent,  $parent_{x_2}$ , for the  $x_{\text{th}}$  mating pair. This selection mechanism is iteratively performed to establish a total of  $MatP$  mating pairs.

As we select the parents, the generation of two offspring per mating pair is obtained through the mating procedure,

---

**Algorithm 1** Genetic Algorithm-Based Solution for Problem P2

---

- 1: **inputs:**  $N_{\text{pop}}, I, SelRate, MutR, \tau, \{R_{k,\text{min}}\}$ .
  - 2: Initialize iteration index  $i = 1$ .
  - 3: Initialize the chromosomes,  $cr_n$ , in the population and solve equation (12a) to get  $f(cr_n)$ .
  - 4: Calculate  $N_{\text{keep}}$ ,  $MatP$ , and  $N_{\text{mut}}$ , and sort the chromosomes in descending order according to cost  $f(cr_n)$ .
  - 5: **while**  $i \leq I$  **do**
  - 6:   Discard  $N_{\text{pop}} - N_{\text{keep}}$  chromosomes.
  - 7:   Create the mating pool to get  $CPb_n, n = 1, \dots, N_{\text{keep}}$ .
  - 8:   **for**  $x = 1, \dots, MatP$  **do**
  - 9:     Select  $parent_1^x$  and  $parent_2^x$  for  $x_{\text{th}}$  mating pair.
  - 10:    Execute the mating process to generate two offspring,  $offsp_1^x$  and  $offsp_2^x$ , by using (16), (17a), (17b), (18a), and (18b).
  - 11:   **end for**
  - 12:   Replace the discarded  $N_{\text{pop}} - N_{\text{keep}}$  chromosomes with the newly generated offspring from the  $MatP$  mating pairs.
  - 13:   Mutate the  $N_{\text{mut}}$  selected variables of the chromosomes using (19).
  - 14:   Evaluate updated population using objective function (12a) and re-sort chromosomes by cost.
  - 15:   Update iteration index:  $i \leftarrow i + 1$ .
  - 16: **end while**
  - 17: **output:** The best chromosome is  $cr_1$  with beamform vector  $f(cr_1)$  and near-optimal values for the variables of problem (12a).
- 

which is predicated on the crossover strategy [53], [54]. For every  $x_{\text{th}}$  mating pair, the crossover point, denoted as  $\{\psi_x\}$ , is ascertained by randomly selecting one of the variables from the parents within the  $x_{\text{th}}$  mating pair. The crossover point is determined as follows:

$$\psi_x = \lceil rand_{x,\text{mat}} \times N_{\text{var}} \rceil, \quad (16)$$

This ensures the crossover point is within the range of the chromosome's variables, and we define  $rand_{x,\text{mat}}$  as a random number between  $[0, 1]$ . Then, new variables are created in the following manner for the two offspring of the  $x_{\text{th}}$  mating pair by combining variables for  $\psi_x$  from the parents:

$$v_{\psi_x}^{\text{new1},x} = v_{\psi_x}^{\text{parent}_1^x} - \varepsilon_x \left( v_{\psi_x}^{\text{parent}_1^x} - v_{\psi_x}^{\text{parent}_2^x} \right), \quad (17a)$$

$$v_{\psi_x}^{\text{new2},x} = v_{\psi_x}^{\text{parent}_2^x} + \varepsilon_x \left( v_{\psi_x}^{\text{parent}_1^x} - v_{\psi_x}^{\text{parent}_2^x} \right), \quad (17b)$$

where  $v_{\psi_x}^{\text{parent}_j^x}$  represents the value of variable  $\psi_x$  associated with the  $j_{\text{th}}$  parent, while  $\varepsilon_x$  denotes a random number selected from the interval  $[0,1]$ , as illustrated in [55]. Consequently, offspring from the  $x_{\text{th}}$  mating pair are produced through the following procedure:

$$offsp_1^x = \left[ v_1^{\text{parent}_1^x}, \dots, v_{\psi_x}^{\text{new1},x}, \dots, v_{\psi_x+1}^{\text{parent}_2^x}, \dots, v_{N_{\text{var}}}^{\text{parent}_2^x} \right], \quad (18a)$$

$$\text{offsp}_2^x = \left[ v_1^{\text{parent}_2^x}, \dots, v_{\psi_x}^{\text{new}2,x}, \dots, v_{\psi_x+1}^{\text{parent}_1^x}, \dots, v_{N_{\text{var}}}^{\text{parent}_1^x} \right]. \quad (18b)$$

where  $\text{offsp}_1^x$  and  $\text{offsp}_2^x$  denote the pair of progeny derived from the  $x_{\text{th}}$  mating pair. Consequently, this methodology facilitates the generation of  $N_{\text{pop}} - N_{\text{keep}}$  offspring, designed to replace the same number of chromosomes eliminated during the initial selection phase.

To this end, an elitism strategy is implemented, ensuring that the best solutions found in the population are retained unaltered. Specifically, the top two chromosomes, denoted as  $N_{\text{elit}} = 2$ , are preserved without modification, thereby preventing their loss through mutation or crossover operations. The adaptive mutation mechanism is applied to the remaining chromosomes, with the exception of the elite ones. This equation determines the total number of mutations carried out:

$$N_{\text{mut}} = \text{round}((N_{\text{pop}} - N_{\text{elit}})N_{\text{var}}\text{MutR}) \quad (19)$$

where  $(N_{\text{pop}} - N_{\text{elit}})N_{\text{var}}$  denotes the variables that can undergo mutation throughout the population, and  $\text{MutR}$  is the predetermined mutation rate. This formula calculates the aggregate mutations across the population, factoring in the number of mutable genes post-elitism. During the mutation, a chromosome and a specific gene within it are randomly selected. Mutation involves modifying the gene's value by incorporating a Gaussian noise component, which is given as

$$v'_{n,i} = v_{n,i} + \Delta(\text{generation}, \sigma) \quad (20)$$

where  $v'_{n,i}$  denotes the mutated value of gene  $i$  in chromosome  $n$ , with  $v_{n,i}$  being its original value. The term  $\Delta(\text{generation}, \sigma)$  represents Gaussian noise with standard deviation  $\sigma$ , which diminishes as the generation number increases. The magnitude of this noise is calculated as  $\sigma = 0.2 + \frac{\text{adaptiveMutationFactor}}{\text{generation}}$ . This adaptive approach ensures that mutations are more prominent in initial generations to facilitate exploration, and they gradually decrease to promote exploitation as the algorithm approaches convergence.

## 2) THE INNER-LEVEL SUB-PROBLEM SOLUTION USING A LAGRANGIAN METHOD

In this sub-problem, we address the optimization of downlink and uplink time allocations  $\boldsymbol{\tau} = \{\tau_0, \tau_1, \tau_2, \dots, \tau_k\}$  in Problem P3 while keeping beamforming vector  $\mathbf{w}$  constant. Given that Problem P3 is characterized as a convex optimization problem that can be solved using convex optimization, we consider the Lagrange multiplier technique to solve it. The Lagrange multiplier method finds the local maxima and minima of a function while satisfying equality constraints. The formulation of the Lagrangian function for solving Problem P3 is as follows:

$$\mathcal{L}_{\text{sum}}(\boldsymbol{\tau}, \lambda) = \sum_{k=1}^K \tau_k \log_2 \left( 1 + C_k \frac{\tau_0}{\tau_k} \right) + \lambda \left( 1 - \sum_{k=1}^K \tau_k \right), \quad (21)$$

### Algorithm 2 Lagrange Optimization and the Newton-Raphson-Based Algorithm to Solve Problem P3

- 1: Initialize  $\lambda$ ,  $\tau_0$ ,  $\tau_k$ , and  $w_0$ .
- 2: **repeat**
- 3:   Solve Problem P3 using (26) & (27) and find optimal values for  $\{\tau_0^*, \{\tau_k^*\}\}$ .
- 4:   Compute  $\mathcal{D}(\lambda)$  using (21) and check for the feasible solution.
- 5:   Compute  $\mathcal{D}(\lambda)$  as the minimum of  $\mathcal{L}_{\text{sum}}(\boldsymbol{\tau}, \lambda)$  over the feasible set  $\mathcal{S}$  according to (22).
- 6:   Update  $\lambda$  using the sub-gradient method
- 7:   **if**  $|\lambda - \lambda_{\text{old}}| < \epsilon$  **then**
- 8:     Convergence achieved, exit loop.
- 9:   **end if**
- 10:   Set  $\lambda_{\text{old}} = \lambda$
- 11: **until** Stopping criterion is met
- 12: **output:** Optimal time allocations  $\tau_0^*, \tau_k^*$  and optimal Lagrange multiplier  $\lambda^*$ .

$$\text{where, } C_k = \frac{\sum_{n=1}^N \xi_{k,n} \|\mathbf{h}_{k,n}^H \mathbf{w}\|^2 \|\mathbf{h}_{k,n}\|^2}{\sigma^2}.$$

After formulating the Lagrangian for the primal problem, where  $\lambda \geq 0$  represents the Lagrange multiplier associated with constraint (13b). The dual function for Problem P3 is

$$\mathcal{D}(\lambda) = \min_{\boldsymbol{\tau} \in \mathcal{S}} \mathcal{L}_{\text{sum}}(\boldsymbol{\tau}, \nu), \quad (22)$$

where  $\mathcal{S}$  is the feasible set of  $\boldsymbol{\tau}$  as seen in (13b), which shows that  $\boldsymbol{\tau} \in \mathcal{S}$  with  $\tau_k > 0, k = 0, 1, \dots, K$ . Given that Problem P3 is a convex optimization problem where strong duality holds, the Karush-Kuhn-Tucker (KKT) conditions serve as necessary and sufficient criteria for its global optimality, which are given by

$$\sum_{k=0}^K \tau_k^* \leq 1, \quad (23)$$

$$\lambda^* \left( \sum_{k=0}^K \tau_k^* - 1 \right) = 0, \quad (24)$$

$$\frac{\partial}{\partial \tau_k} \mathcal{R}_{\text{sum}}(\boldsymbol{\tau}^*) - \lambda^* = 0, \quad k = 0, 1, 2, \dots, K. \quad (25)$$

Let  $\tau_k^*$  and  $\lambda^*$  denote the optimal primal and dual solutions, respectively, of Problem P3. Therefore, without loss of generality, we assume  $\lambda^* > 0$ . Hence, optimal time allocation solution  $\{\tau_0^*, \{\tau_k\}^*\}$  is given by

$$\tau_0^* = \frac{1}{1 + \sum_{k=1}^K \eta_k^*} \quad (26)$$

$$\tau_i^* = \frac{\eta_i^*}{1 + \sum_{k=1}^K \eta_k^*}, \quad \forall k \quad (27)$$

where  $\eta_k^*$  can be found by solving the KKT conditions of the Lagrangian function in (21), as described in [56]. With feasible optimal solution  $\{\tau_0^*, \{\tau_k\}^*\}$ , we update  $\lambda$  using

the sub-gradient method and iteratively solve for  $\lambda^*$  when convergence is achieved. To find  $\eta_k^*$ , we use the Newton-Raphson method, which is known for its efficiency in solving non-linear equations. The time allocation procedure is summarized in Algorithm 2.

Hence, the complete algorithm for solving Problem P1 is presented in Algorithm 3, and a flow chart for its graphical representation is Fig. 3.

---

**Algorithm 3** The Genetic Algorithm and Lagrangian Optimization to Solve Problem P1

---

- 1: **Initialization:** Set initial values for  $w_0$ ,  $\tau_0$ , and  $\{\tau_k\}$ .
  - 2: Set  $I = 0$  and  $R^{(0)} = f(w_0, \tau_0, \{\tau_k\})$ .
  - 3: **repeat**
  - 4:   Set  $I = I + 1$
  - 5:   Under given  $\tau_0$  and  $\{\tau_k\}$ , update  $w_0$  by solving problem (P2).
  - 6:   Under given  $w_0$ , update  $\tau_0$  and  $\{\tau_k\}$  by solving problem (P3).
  - 7:   Set  $R^{(I)} = f(w_0, \tau_0, \{\tau_k\})$
  - 8: **until**  $\frac{|R^{(I)} - R^{(I-1)}|}{R^{(I)}} < \epsilon$
- 

### 3) COMPLEXITY ANALYSIS

This study examined the computational complexity of Algorithm 3. Problem P1 was solved using a Bi-level programming method, where GA used to optimize the beamforming vectors in the outer problem, with an inner problem solved via Lagrangian method. The computational complexity is expressed as:

$$\mathcal{O}((N_{pop} - N_{elit}) \cdot I \cdot C_{lgr})$$

where  $N_{pop}$  represents the total number of population,  $N_{elit}$  denotes the elitism, which are carried over to the next generation without undergoing genetic operations such as crossover or mutation.  $I$  is the number of iterations the GA performs throughout the optimization process.  $C_{lgr}$  denotes the computational complexity associated with solving the inner problem using Lagrangian relaxation for each individual solution during each iteration. This complexity formula reflects the worst-case scenario, where every non-elite individual in each generation requires a full computation of the inner problem using Lagrangian methods, compounded over all iterations of the GA.

## IV. NUMERICAL RESULTS AND DISCUSSION

To evaluate the performance of the proposed hybrid NOMA-TDMA approach in WPINs, simulations were conducted using MATLAB R2022b by running approximately 100 iterations on a computer with an AMD Ryzen 5 5600X processor at 3.70 GHz with six cores and 12 threads. The experiments considered a distance-dependent path loss channel model expressed as  $H = 10^{-3}d^{-\alpha}$  where  $\alpha$  is the path loss exponent. We chose  $\alpha = 3$  for our simulations. Other key parameters included the total transmit power budget at the hybrid access point, set to  $P_{max} = 30dBm$ ,

efficiency of energy harvesting set at  $\zeta_n = \zeta = 0.8$ , and noise variance set at  $\sigma^2 = -70dBm/Hz$ . Additionally, IoT users were assumed to be uniformly distributed at one to two meters from the BS.

In this paper, we considered baseline schemes for optimized OMA (i.e., TDMA) and for fixed time with optimal  $w_0$  and ETA (i.e., a fixed time and a random  $w_0$ ). Fig. 4 provides a convergence analysis of the proposed genetic algorithm showing an upward trend corresponding to the increase in the number of iterations. Moreover, an increasing trend is observed in the value for best costs as the number of transmit antennae ( $M$ ) increases. The GA parameters were set as follows: population size  $N_{pop} = 20$ , selection rate  $Sel_{Rate} = 0.2$ , mutation rate  $MutR = 0.5$ , maximum iterations at  $I_{max} = 100$ , and adaptive mutation control factor  $adpt = 0.001$ . From Fig. 4, observe that with those specified settings, the GA effectively converges to near-optimal values. This convergence analysis validates the effectiveness and efficiency of our proposed method in achieving near-optimal solutions for the hybrid NOMA-TDMA-based wireless powered IoT network, and helped improve network performance.

Fig. 5 shows the relationship between sum throughput and the number of antennae ( $M$ ) at the H-AP. This graph shows that as the number of antennae at the H-AP increases, a more efficient beamforming design can be achieved, thereby increasing the sum throughput. Moreover, observe from the figure that the proposed scheme with optimal time allocation  $\tau$  and beamforming vectors  $w_0$  performed better than the other schemes, i.e., optimized orthogonal multiple access (OMA) throughput, with a fixed  $\tau$  with optimal  $w_0$ , and with a fixed  $\tau$  with random  $w_0$  employing equal time allocation. Our proposed scheme with optimal  $\tau$  and  $w_0$  consistently achieved the highest sum throughput across all antennae counts, demonstrating superior performance relative to other methods. The OMA throughput and scenario with fixed  $\tau$  and optimal beamforming vector  $w_0$  showed throughput improvement with increases in the number of transmit antennae, but it could not surpass the proposed method's performance. In addition, the scenario with ETA was consistently the least effective, demonstrating the lowest throughput across the different values for  $M$ . Overall, the graph suggests the effectiveness of transmit antennae at the H-AP for sum throughput.

Fig. 6 illustrates sum throughput as a function of the number of user groups ( $K$ ) in a hybrid NOMA-TDMA system. This system configuration involves random distribution of a total of  $N_t = 12$  users with  $K = 2, 3, 4$ , and  $6$ , resulting in  $N = N_t/K$  users in each group and transmit antennae  $M=4$ . We see that for more groups of users, higher throughput can be achieved. This is because with more groups there are more degrees of freedom for both beamforming and time allocation optimization, which results in higher sum throughput. The proposed scheme, employing optimal time allocation  $\tau$  and beamforming vectors  $w_0$  provided a notable enhancement in system throughput as the number of

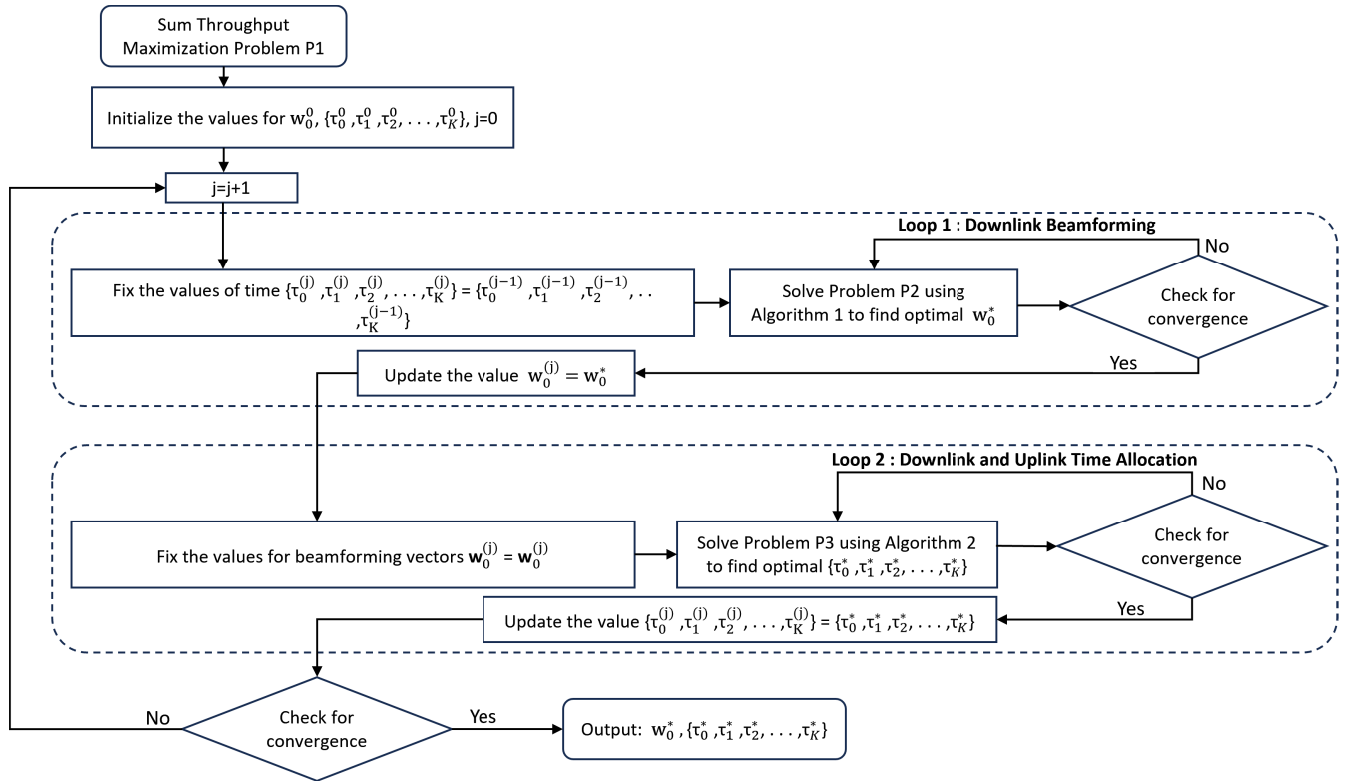


FIGURE 3. The flowchart for solving Problem P1.

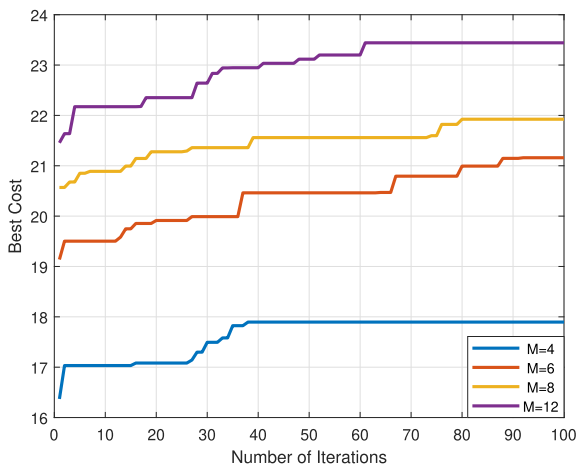


FIGURE 4. Convergence of the genetic algorithm for different values of M.

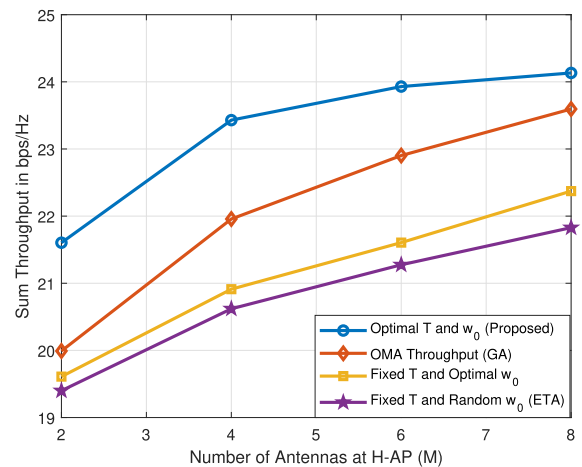


FIGURE 5. Sum throughput for different numbers of H-AP antennae (M).

groups increased. In contrast, the fixed-time techniques, with both optimal and random beamforming vectors, displayed throughput improvements but did not achieve performance levels superior to the proposed adaptive strategy.

Fig. 7 shows the relationship between sum throughput and the number of users,  $N$ , confirming a direct relationship between throughput and users across various operational scenarios, because individual user rates are cumulatively added to system throughput. We considered  $N = 2, 4, 6$ , and  $8$ , with the number of transmit antennae at  $M=4$ .

Notably, implementation of the proposed method, which optimizes both time allocation  $\tau$  and beamforming vectors  $\mathbf{w}_0$ , achieved superior sum throughput, reinforcing a positive link between user density and system performance. In comparison, throughput performance via OMA was worse than under the proposed method. Despite this, the trend remained upward, indicating that traditional access methods similarly benefit from an increase in the number of users. The fixed  $\tau$  strategy with optimized  $\mathbf{w}_0$  exhibited a similar upward trend at consistently lower throughput than the proposed approach, which underscores the value

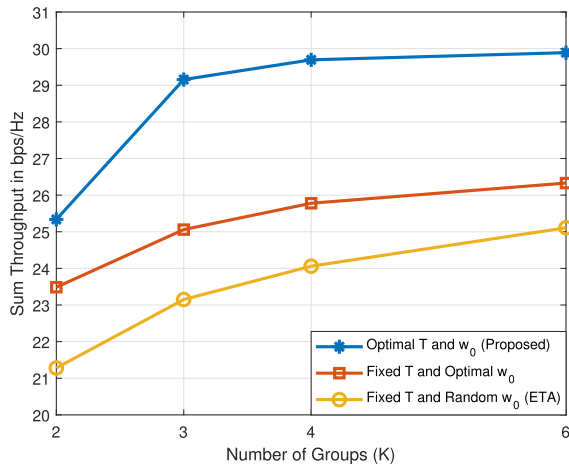


FIGURE 6. Sum throughput with different numbers of groups (K).

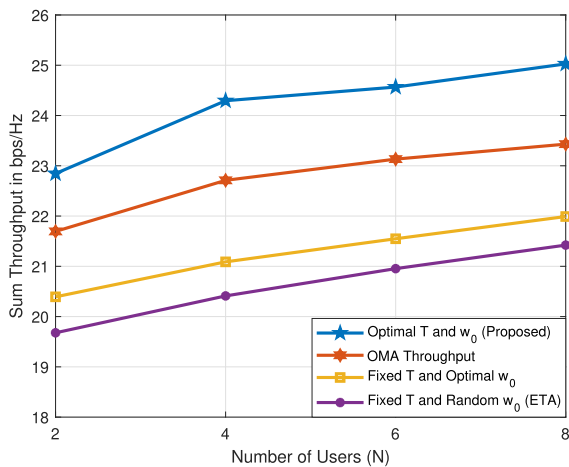


FIGURE 7. Sum throughput with different numbers of users (N).

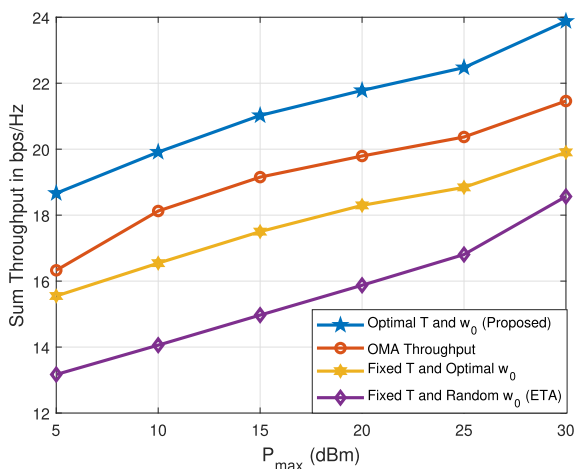


FIGURE 8. Sum throughput from differing maximum available power for transmission.

added by dynamic optimization. The strategy employing ETA illustrated the least improvement in throughput, with only a slight increase as the number of users increased. This underscores the inherent constraints of static strategies in

dynamic user environments, emphasizing the necessity for adaptive optimization to achieve efficient system throughput.

Variations in sum throughput from increasing maximum available transmit power in decibel milliwatts at the H-AP is shown in Fig. 8. The graph illustrates that more available transmit power increases sum throughput because of the freedom in algorithm convergence to find optimal values. In addition, the proposed method outperformed optimal time  $\tau$  and optimal beamforming vectors  $w_0$ , in contrast with the other scenarios.

## V. CONCLUSION

In this paper, we explored a hybrid NOMA-TDMA-based WPIN to enhance sum throughput. We considered bi-level programming to solve the problem. In particular, NOMA and TDMA are used to reduce the complexity of the system, whereas time allocations for downlink and uplink transmissions and downlink beamforming vectors are jointly optimized to maximize the sum throughput of the network. We employ a genetic algorithm and a Lagrangian method to identify an optimal solution characterized by rapid convergence. Subsequent evaluation of simulations revealed that the hybrid approach outperformed alternative scenarios and strategies, improving the system’s sum throughput.

## REFERENCES

- [1] P. Ramezani and A. Jamalipour, “Toward the evolution of wireless powered communication networks for the future Internet of Things,” *IEEE Netw.*, vol. 31, no. 6, pp. 62–69, Nov. 2017.
- [2] R. Hassan, F. Qamar, M. K. Hasan, A. H. M. Aman, and A. S. Ahmed, “Internet of Things and its applications: A comprehensive survey,” *Symmetry*, vol. 12, no. 10, p. 1674, Oct. 2020.
- [3] J. Santos, J. J. P. C. Rodrigues, J. Casal, K. Saleem, and V. Denisov, “Intelligent personal assistants based on Internet of Things approaches,” *IEEE Syst. J.*, vol. 12, no. 2, pp. 1793–1802, Jun. 2018.
- [4] J. A. Khan, H. K. Qureshi, and A. Iqbal, “Energy management in wireless sensor networks: A survey,” *Comput. Electr. Eng.*, vol. 41, pp. 159–176, Jul. 2015.
- [5] R. Wang and D. R. Brown, “Throughput maximization in wireless powered communication networks with energy saving,” in *Proc. 48th Asilomar Conf. Signals, Syst. Comput.*, Nov. 2014, pp. 516–520.
- [6] R. E. Nafiaa and A. Z. Yonis, “Analysis of frequency splitting phenomenon in WPT for intelligent applications,” in *Proc. IEEE Int. Conf. Autom. Control Intell. Syst. (I2CACIS)*, Jun. 2022, pp. 174–179.
- [7] H. Yetgin, K. T. K. Cheung, M. El-Hajjar, and L. H. Hanzo, “A survey of network lifetime maximization techniques in wireless sensor networks,” *IEEE Commun. Surveys Tuts.*, vol. 19, no. 2, pp. 828–854, 2nd Quart., 2017.
- [8] R. E. Nafiaa and A. Z. Yonis, “Performance analysis of high-efficiency WPT for communication technologies,” in *Proc. 14th Int. Conf. Comput. Intell. Commun. Netw. (CICN)*, Dec. 2022, pp. 78–82.
- [9] X. Liu, Z. Qin, Y. Gao, and J. A. McCann, “Resource allocation in wireless powered IoT networks,” *IEEE Internet Things J.*, vol. 6, no. 3, pp. 4935–4945, Jun. 2019.
- [10] S. U. Khan, C. E. García, T. Hwang, and I. Koo, “Radio environment map construction based on privacy-centric federated learning,” *IEEE Access*, vol. 12, pp. 28109–28121, 2024.
- [11] M. Abdullah, M. Ghanim, and A. Yonis, “Effects of FFT size on papr of MC-CDMA system,” in *Proc. IEEE 9th Int. Colloq. Signal Process. Appl.*, Sep. 2013, pp. 182–187.
- [12] N. Deepan and B. Rebekka, “Backscatter-assisted wireless powered communication networks with multiple antennas,” in *Proc. Int. Conf. Wireless Commun. Signal Process. Netw. (WiSPNET)*, Aug. 2020, pp. 135–138.

- [13] A. Afridi, I. Hameed, and I. Koo, "Enhancing sum throughput in wireless powered IoT networks using TDMA-based resource allocation," in *Proc. 26th Int. Conf. Mechatronics Technol. (ICMT)*, Oct. 2023, pp. 1–5.
- [14] G. Yang, C. K. Ho, R. Zhang, and Y. L. Guan, "Throughput optimization for massive MIMO systems powered by wireless energy transfer," *IEEE J. Sel. Areas Commun.*, vol. 33, no. 8, pp. 1640–1650, Aug. 2015.
- [15] S. Zhong and X. Wang, "Energy allocation and utilization for wirelessly powered IoT networks," *IEEE Internet Things J.*, vol. 5, no. 4, pp. 2781–2792, Aug. 2018.
- [16] A. S. Yonis and A. Nawaf, "Investigation of evolving multiple access technologies for 5G wireless system," in *Proc. 8th Int. Eng. Conf. Sustain. Technol. Develop. (IEC)*, Feb. 2022, pp. 118–122.
- [17] W. U. Khan, J. Liu, F. Jameel, V. Sharma, R. Jäntti, and Z. Han, "Spectral efficiency optimization for next generation NOMA-enabled IoT networks," *IEEE Trans. Veh. Technol.*, vol. 69, no. 12, pp. 15284–15297, Dec. 2020.
- [18] G. Yang, X. Xu, and Y.-C. Liang, "Resource allocation in NOMA-enhanced backscatter communication networks for wireless powered IoT," *IEEE Wireless Commun. Lett.*, vol. 9, no. 1, pp. 117–120, Jan. 2020.
- [19] B. Liu, C. Liu, and M. Peng, "Resource allocation for energy-efficient MEC in NOMA-enabled massive IoT networks," *IEEE J. Sel. Areas Commun.*, vol. 39, no. 4, pp. 1015–1027, Apr. 2021.
- [20] Z. Ding, Z. Yang, P. Fan, and H. V. Poor, "On the performance of non-orthogonal multiple access in 5G systems with randomly deployed users," *IEEE Signal Process. Lett.*, vol. 21, no. 12, pp. 1501–1505, Dec. 2014.
- [21] K. Higuchi and A. Benjebbour, "Non-orthogonal multiple access (NOMA) with successive interference cancellation for future radio access," *IEICE Trans. Commun.*, vol. 98, no. 3, pp. 403–414, 2015.
- [22] Q. Wu, W. Chen, D. W. K. Ng, and R. Schober, "Spectral and energy-efficient wireless powered IoT networks: NOMA or TDMA?" *IEEE Trans. Veh. Technol.*, vol. 67, no. 7, pp. 6663–6667, Jul. 2018.
- [23] H. Ju and R. Zhang, "Throughput maximization in wireless powered communication networks," *IEEE Trans. Wireless Commun.*, vol. 13, no. 1, pp. 418–428, Jan. 2014.
- [24] D. K. P. Asiedu, S. Mahama, C. Song, D. Kim, and K.-J. Lee, "Beamforming and resource allocation for multiuser full-duplex wireless-powered communications in IoT networks," *IEEE Internet Things J.*, vol. 7, no. 12, pp. 11355–11370, Dec. 2020.
- [25] Z. Yang, W. Xu, Y. Pan, C. Pan, and M. Chen, "Optimal fairness-aware time and power allocation in wireless powered communication networks," *IEEE Trans. Commun.*, vol. 66, no. 7, pp. 3122–3135, Jul. 2018.
- [26] K. Zheng, R. Luo, Z. Wang, X. Liu, and Y. Yao, "Short-term and long-term throughput maximization in mobile wireless-powered Internet of Things," *IEEE Internet Things J.*, vol. 11, no. 6, pp. 10575–10591, Mar. 2024.
- [27] R. Rezaei, S. Sun, X. Kang, Y. L. Guan, and M. R. Pakravan, "Secrecy throughput maximization for full-duplex wireless powered IoT networks under fairness constraints," *IEEE Internet Things J.*, vol. 6, no. 4, pp. 6964–6976, Aug. 2019.
- [28] C. Yang, X. Wang, and K.-W. Chin, "On max–min throughput in backscatter-assisted wirelessly powered IoT," *IEEE Internet Things J.*, vol. 7, no. 1, pp. 137–147, Jan. 2020.
- [29] T. A. Zewde and M. C. Gursoy, "NOMA-based energy-efficient wireless powered communications," *IEEE Trans. Green Commun. Netw.*, vol. 2, no. 3, pp. 679–692, Sep. 2018.
- [30] D. Zhai, R. Zhang, L. Cai, B. Li, and Y. Jiang, "Energy-efficient user scheduling and power allocation for NOMA-based wireless networks with massive IoT devices," *IEEE Internet Things J.*, vol. 5, no. 3, pp. 1857–1868, Jun. 2018.
- [31] A. Rauniyar, P. Engelstad, and O. Østerbø, "RF energy harvesting and information transmission based on NOMA for wireless powered IoT relay systems," *Sensors*, vol. 18, no. 10, p. 3254, Sep. 2018.
- [32] J. Wang, X. Kang, S. Sun, and Y.-C. Liang, "Throughput maximization for peer-assisted wireless powered IoT NOMA networks," *IEEE Trans. Wireless Commun.*, vol. 19, no. 8, pp. 5278–5291, Aug. 2020.
- [33] S. A. Tegos, P. D. Diamantoulakis, A. S. Lioumpas, P. G. Sarigiannidis, and G. K. Karagiannidis, "Slotted Aloha with NOMA for the next generation IoT," *IEEE Trans. Commun.*, vol. 68, no. 10, pp. 6289–6301, Oct. 2020.
- [34] M. Ahmed, W. U. Khan, A. Ihsan, X. Li, J. Li, and T. A. Tsiftsis, "Backscatter sensors communication for 6G low-powered NOMA-enabled IoT networks under imperfect SIC," *IEEE Syst. J.*, vol. 16, no. 4, pp. 5883–5893, Dec. 2022.
- [35] H. Al-Obiedollah, K. Cumanan, A. G. Burr, J. Tang, Y. Rahulamathavan, Z. Ding, and O. A. Dobre, "On energy harvesting of hybrid TDMA-NOMA systems," in *Proc. IEEE Global Commun. Conf. (GLOBECOM)*, Dec. 2019, pp. 1–6.
- [36] S. Khavari-Moghaddam, S. Farahmand, S. M. Razavizadeh, and I. Lee, "Optimum solutions for weighted sum-rate of NOMA and TDMA in wireless-powered IoT networks," *IEEE Internet Things J.*, vol. 11, no. 2, pp. 3302–3315, Jan. 2024.
- [37] D. Zhang, Q. Wu, M. Cui, G. Zhang, and D. Niyato, "Throughput maximization for IRS-assisted wireless powered hybrid NOMA and TDMA," *IEEE Wireless Commun. Lett.*, vol. 10, no. 9, pp. 1944–1948, Sep. 2021.
- [38] X. Chen, D. Xu, and H. Zhu, "Cooperative resource allocation for hybrid NOMA-OMA-based wireless powered MC-IoT systems with hybrid relays," *Electronics*, vol. 13, no. 1, p. 99, Dec. 2023.
- [39] H. Qi, Y. Peng, and H. Zhang, "Performance analysis for wireless-powered IoT networks with hybrid non-orthogonal multiple access," *J. Smart Environ. Green Comput.*, vol. 2, no. 3, pp. 105–125, 2022.
- [40] Y. Zhu, X. Yuan, Y. Hu, T. Wang, M. C. Gursoy, and A. Schmeink, "Low-latency hybrid NOMA-TDMA: QoS-driven design framework," *IEEE Trans. Wireless Commun.*, vol. 22, no. 5, pp. 3006–3021, May 2023.
- [41] D.-H. Chen and E.-H. Jiang, "Joint power and time allocation in hybrid NOMA/OMA IoT networks for two-way communications," *Entropy*, vol. 24, no. 12, p. 1756, 2022.
- [42] S. Mounchili and S. Hamouda, "New user grouping scheme for better user pairing in NOMA systems," in *Proc. Int. Wireless Commun. Mobile Comput. (IWCMC)*, Jun. 2020, pp. 820–825.
- [43] S. Arif, M. A. Khan, and S. U. Rehman, "Wireless channel estimation for low-power IoT devices using real-time data," *IEEE Access*, vol. 12, pp. 17895–17914, 2024.
- [44] P. Liu and T. Jiang, "Channel estimation performance analysis of massive MIMO IoT systems with Ricean fading," *IEEE Internet Things J.*, vol. 8, no. 7, pp. 6114–6126, Apr. 2021.
- [45] Y. Qiang, X. Shao, and X. Chen, "A model-driven deep learning algorithm for joint activity detection and channel estimation," *IEEE Commun. Lett.*, vol. 24, no. 11, pp. 2508–2512, Nov. 2020.
- [46] J. Zhang and M. Han, "Secrecy analysis for IoT relaying networks deploying NOMA with energy harvesting," *J. Franklin Inst.*, vol. 358, no. 18, pp. 10232–10249, Dec. 2021. [Online]. Available: <https://www.sciencedirect.com/science/article/pii/S0016003221006037>
- [47] A. Shome, A. K. Dutta, and S. Chakrabarti, "Throughput assessment of non-linear energy harvesting secondary IoT network with hardware impairments and randomly located licensed users in Nakagami- $m$  fading," *IEEE Trans. Veh. Technol.*, vol. 70, no. 7, pp. 7283–7288, Jul. 2021.
- [48] H.-T. Ye, X. Kang, J. Joung, and Y.-C. Liang, "Optimization for full-duplex rotary-wing UAV-enabled wireless-powered IoT networks," *IEEE Trans. Wireless Commun.*, vol. 19, no. 7, pp. 5057–5072, Jul. 2020.
- [49] X. Kang, C. K. Ho, and S. Sun, "Full-duplex wireless-powered communication network with energy causality," *IEEE Trans. Wireless Commun.*, vol. 14, no. 10, pp. 5539–5551, Oct. 2015.
- [50] D.-T. Do, T.-L. Nguyen, S. Ekin, Z. Kaleem, and M. Voznak, "Joint user grouping and decoding order in uplink/downlink MISO/SIMO-NOMA," *IEEE Access*, vol. 8, pp. 143632–143643, 2020.
- [51] I. Hameed, M. R. Camana, P. V. Tuan, and I. Koo, "Intelligent reflecting surfaces for sum-rate maximization in cognitive radio enabled wireless powered communication network," *IEEE Access*, vol. 11, pp. 16021–16031, 2023.
- [52] H. Guo, B. Makki, and T. Svensson, "A genetic algorithm-based beamforming approach for delay-constrained networks," in *Proc. 15th Int. Symp. Modeling Optim. Mobile, Ad Hoc, Wireless Netw. (WiOpt)*, May 2017, pp. 1–7.
- [53] S. Mirjalili, "Genetic algorithm," in *Evolutionary Algorithms and Neural Networks: Theory and Applications*. Cham, Switzerland: Springer, 2019, ch. 4, pp. 43–55.
- [54] R. L. Haupt and S. E. Haupt, *Practical Genetic Algorithms*. Hoboken, NJ, USA: Wiley, 2004.
- [55] M. R. Camana, C. E. Garcia, and I. Koo, "Rate-splitting multiple access in a MISO SWIPT system assisted by an intelligent reflecting surface," *IEEE Trans. Green Commun. Netw.*, vol. 6, no. 4, pp. 2084–2099, Dec. 2022.
- [56] I. Hameed and I. Koo, "Max-min throughput optimization in WPCNs: A hybrid active/passive IRS-assisted scheme," *IEEE Open J. Commun. Soc.*, vol. 5, pp. 1123–1140, 2024.



**ABID AFRIDI** received the B.E. degree in electrical engineering (telecommunication) from the University of Science and Technology Bannu, Bannu, Pakistan, in 2020. He is currently a Graduate Research Assistant with the Department of Electrical, Electronic and Computer Engineering, University of Ulsan, Ulsan, South Korea. His research interests include the wireless powered IoT networks, optimization, and intelligent reflecting surfaces.



**CARLA E. GARCÍA** (Member, IEEE) received the B.Eng. degree in electronics and telecommunications engineering from Escuela Politécnica Nacional (EPN), Quito, Ecuador, in 2016, and the M.Sc. and Ph.D. degrees from the University of Ulsan, South Korea, in 2020 and 2023, respectively. She was awarded the Brain Korean (BK) 21+ Scholarship for her masters and Ph.D. studies in South Korea. She held the positions of a Research Assistant and a Postdoctoral Researcher with the Department of Electrical, Electronic and Computer Engineering, University of Ulsan, South Korea. She joined the Interdisciplinary Centre for Security, Reliability and Trust (SnT), University of Luxembourg, Luxembourg, where she is currently a Research Associate.



**IQRA HAMEED** received the B.E. and M.E. degrees in electrical engineering from the University of Engineering and Technology at Lahore, Lahore, Pakistan, in 2013 and 2017, respectively, and the Ph.D. degree from the Department of Electrical, Electronic and Computer Engineering, University of Ulsan, Ulsan, South Korea, in 2024. She is currently a Postdoctoral Fellow with Hanyang University, Seoul, South Korea. Her research interests include wireless powered communications networks, deep learning, and optimization.



**INSOO KOO** received the B.E. degree from Konkuk University, Seoul, South Korea, in 1996, and the M.Sc. and Ph.D. degrees from Gwangju Institute of Science and Technology (GIST), Gwangju, South Korea, in 1998 and 2002, respectively. From 2002 to 2004, he was a Research Professor with the Ultrafast Fiber-Optic Networks Research Center, GIST. In 2003, he was a Visiting Scholar with the KTH Royal Institute of Science and Technology, Stockholm, Sweden. In 2005, he joined the University of Ulsan, Ulsan, South Korea, where he is currently a Full Professor. His research interests include spectrum sensing issues for CRNs, channel and power allocation for cognitive radio (CR) and military networks, SWIPT MIMO issues in CR, MAC, routing protocol design for UW-ASNs, and relay selection issues in CCRNs.

...